

# Investigating the Late Pleistocene to Present-Day Deposition Processes of Paleofloods in the Yellow River-Huangshui River Valley through End-Member Modeling

Zhaokang Zhang<sup>1, 2, 3, a</sup>, Yongjuan Sun<sup>1, 2, 3, b, \*</sup>, Manping Sun<sup>1, 2, 3, c</sup>, Yongxin Zeng<sup>1, 2, 3, d</sup>, Chongyi E<sup>1, 2, 3, e</sup>

<sup>1</sup>Key Laboratory of Tibetan Plateau Land Surface Processes and Ecological Conservation (Ministry of Education), Qinghai Normal University, Xining 810008;

<sup>2</sup> Qinghai Province Key Laboratory of Physical Geography and Environmental Process, College of Geographical Science, Qinghai Normal University, Xining 810008,

China;

<sup>3</sup> Academy of Plateau Science and Sustainability, People's Government of Qinghai Province and Beijing Normal University, Xining 810016, China.

<sup>a</sup>ZZK199818@163.com, <sup>b</sup>yongjuansun@163.com, <sup>c</sup>smp13195796958@163.com, <sup>d</sup>zyx17745475617@163.com, <sup>e</sup>echongyi@163.com

**Abstract.** Detailed field investigations in the Yellow River-Huangshui River Valley(YHV) uncover stratigraphic sections of soil sediments intercalated with multiple layers of slack water deposit(SWD). In-depth analysis of palaeoflood sediment sections in the YHV: Combination of detailed observational measurements, stratigraphic delineation, sampling, optical stimulated luminescence(OSL) dating, grain size analysis, and End-Member(EM) analysis. Non-Parametric method resolves 7 EMs components with distinct source and depositional dynamics from the palaeoflood sediment sequence in 3 sections. Analysis of soil sediment stratigraphic units in the YHV reveals mixed superposition of multiple EM components. Macroscopic characteristics, physical and chemical properties indicate occurrence of paleofloods in 28.9 ka-18.4 ka phases, with SWD formed from long-distance transport of surface sediment carried by river floods and sandy sediment from river diffuse beaches under hydrodynamic action. EM analysis of full sample size reflects diverse sediment dynamics of the YHV. Findings hold significant implications for disaster prevention and mitigation in the region.

**Keywords:** paleoflood; End-Member analysis; optical stimulated luminescence dating.

## 1. Introduction

Investigating the impact of paleofloods on the Yellow River-Huangshui River Valley(YHV): a vital step for disaster prevention and mitigation.

The YHV on the northeastern edge of the Qinghai-Tibet Plateau is one of the most densely populated areas on the plateau, with a large concentration of population, towns, and economic activities[1]. The valley accounts for 72.77% of the population and 60% of the arable land in Qinghai Province, with the majority of the population and economy situated in the flood-prone alluvial plains of the valley[2]. Given the high risk of natural disasters and the threat they pose to life and property, as well as to engineering construction in the area, a better understanding of super-long-scale storm floods in the YHV is crucial[3].

Previous studies have revealed that geochemical elements can provide insight into the source of sediment[4], while the grain size characteristics can shed light on the intensity of hydrodynamic forces acting on the sediment during deposition and its source. The End-member modelling analysis (EMMA) presents advantages over conventional particle size frequency distribution methods[5]. Firstly, it utilizes high precision particle size data more effectively. Secondly, it allows for the separation and individual characterization of each component from a multi-component mixture, thus providing a deeper understanding of the depositional dynamics of the particle size component. The analysis of sediment grain size is a crucial tool for understanding the depositional environment and

the dynamics of sediment transport. The EMMA approach can be used to identify and isolate sensitive grain size components from a sediment sample[6], offering valuable insights into the evolution of regional paleoclimate and paleoenvironment[7].

The EMMA is a widely applied technique for the investigation of sediment depositional processes. While conventional paleoflood identification methods rely on the direct classification of paleoflood periods based on individual indicator curves, this approach is prone to errors in the data and subjective human biases. The current study employs EMMA to calculate the number and distribution of end-members from the covariance matrix of the overall data, and combines this information with an understanding of river evolution and regional geology to develop an end-member model that effectively identifies paleoflood periods. This approach has been successfully applied in the study of wind-borne sediments and has shown great potential for resolving complex sediment dynamics. EMMA has been utilized in the analysis of marine, lake, and eolian sediment sections[8], yielding successful results in determining the source and depositional processes of these materials[9]. The application of EMMA to slack water deposit (SWD) samples in the YHV provides an efficient method for separating out individual sediment dynamics components and identifying their unique characteristics[10].

To grasp the scale and pattern of these events, historical and prehistoric storm flood hydrological data is necessary. In cases where historical records are missing or incomplete, studying the riparian loess-paleosol stratigraphic sequence from the perspective of paleoflood hydrology, combined with optically stimulated luminescence(OSL)[11] and radiocarbon accelerator mass spectrometry(AMS)  $^{14}\text{C}$  dating[12], can help identify and date river flood events. This provides critical data for water resources development and utilization, and flood prevention and mitigation in the river basin.

This study is based on the analysis of sediment grain size and OSL dating in the QSW, YSC and TG-HJ sections in the YHV, and considers the EMMA of multiple complex dynamics to resolve the possible sediment dynamics components of different soil sediment stratigraphic units in the study sections, to interpret the significance of sediment dynamics indicated by sediment grain size in each soil sediment stratigraphic unit, and to further understand the changes in surface processes recorded in the soil sediment stratigraphic sequences of the study sections.

## 2. Study area and sampling strategy

### 2.1 Study area

The Yellow River-Huangshui River Valley (YHV) located between  $35^{\circ}$  to  $38^{\circ}$  N and  $100^{\circ}$  to  $103^{\circ}$  E is situated at the juncture between the Qinghai-Tibet Plateau and Loess Plateau(Fig. 1). The area is known for its ecological sensitivity[13], interspersed agriculture, and pastoral lands and features a plateau arid to semi-arid continental climate with significant variability in precipitation throughout the year. The region is home to numerous tributaries with a dendritic to plume-like water system distribution, where most rivers are seasonal and influenced by rainfall. The YHV is characterized by limited water resources and prevalent sand, with uneven rainfall distribution across the region, increasing with altitude from 300-400 mm in the low-lying shallow mountain and Chuanshui areas to 400-600 mm in higher-altitude mountainous areas[14]. The average annual evaporation from the water surface in the region is 889.3 mm, declining with increasing altitude and exhibiting a southeast-to-northwest gradient in reduction[15].

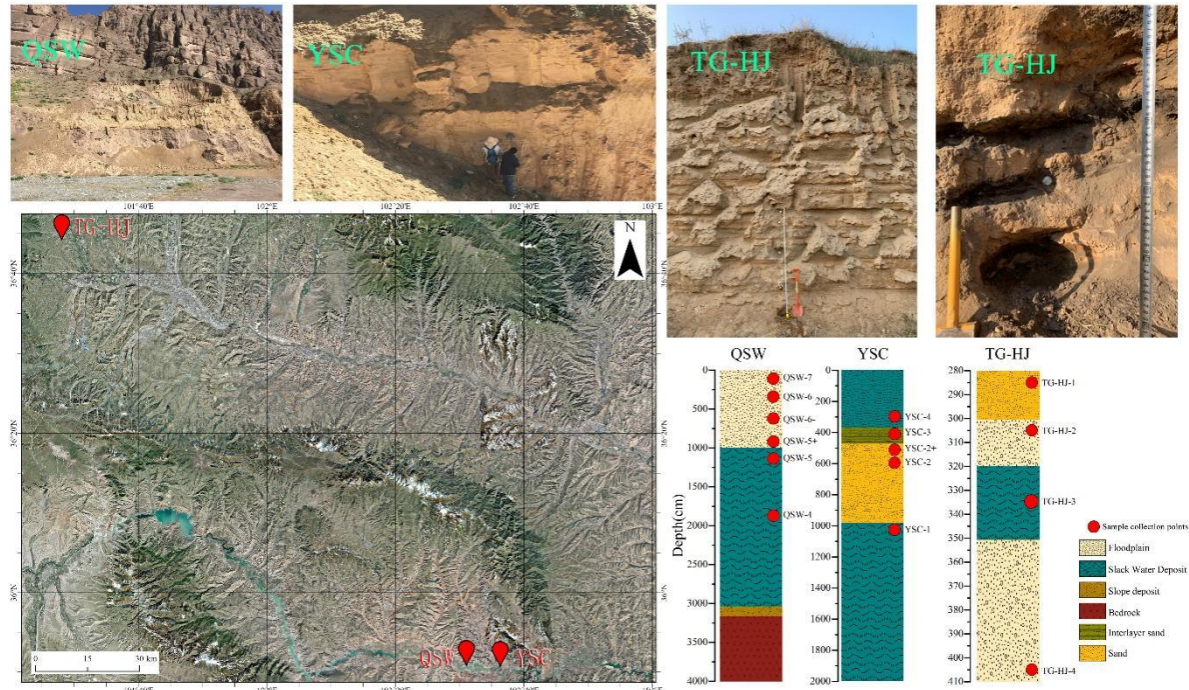


Fig. 1 Location and topography of the Yellow River-Huangshui River Valley (YHV) and the sampling sites

## 2.2 Sampling strategy

During the field investigation, paleoflood sediment layers were identified in 3 sections along the YHV. The sections were named QSW, YSC, and TG-HJ. Analysis of the sediment grain size showed that the QSW section comprised of a floodplain layer (0-1000cm), a SWD layer (1000-3000cm), a slope deposit layer (3000-3200cm), and a bedrock layer (3200-4000cm). The YSC section was found to contain a SWD layer (0-380cm), an interlayer sand layer (380-490cm), a sand layer (490-990cm), and another SWD layer (990-2000cm).

The TG-HJ section was comprised of a sand layer (280-300cm), a floodplain layer (300-320cm), a SWD layer (320-350cm), and another floodplain layer (350-410cm). 4 OSL dating samples were taken from the SWD and adjacent sediment layers of each section, and 15 samples were analyzed for grain size.

## 3. Methods

### 3.1 OSL dating

The OSL dating process involved collecting 4 samples from the sedimentation section, which were treated in a dark room and purified of organic matter and carbonates through a combination of hydrogen peroxide and hydrochloric acid. Quartz grains were extracted from the samples through etching with hydrofluoric acid[16].

The equivalent dose of extracted quartz,  $D_e$ , was calculated using the single aliquot regenerative-dose method, and the water content and U, Th, and K content of the samples were measured by neutron activation analysis[17]. Finally, the photoluminescence dating of the samples was carried out at the Qinghai Provincial Key Laboratory of Physical Geography and Environmental Processes at Qinghai Normal University.

### 3.2 Grain size analysis

The samples underwent a series of processing steps to remove organic matter and carbonates. First, they were dried at a temperature of 30 °C. Then, 5% hydrogen peroxide and 0.2 mol/L

hydrochloric acid were added and heated and boiled, followed by being filled with deionized water and left to settle for 24 hours[18]. The solution was removed from the water, mixed with 0.05 mol/L sodium hexametaphosphate reagent, and sonicated[19].

After shaking for 10-15 minutes to disperse the sample, it was cooled for particle size determination. The particle size measurements were performed using a Mastersizer 2000 laser particle size tester[20] with a range of 0.02-2000  $\mu\text{m}$  and an error of less than 2% at the Qinghai Provincial Key Laboratory of Physical Geography and Environmental Processes, Qinghai Normal University.

## 4. Result

### 4.1 Chronological framework

The results of the OSL dating analysis of the TG-HJ section are reported in Table 1. The results of the analysis show that the sediments in these sections were deposited between  $28.9 \pm 4.9\text{ka}$  to  $18.4 \pm 1.1\text{ka}$ .

The dating results are consistent with the expected stratigraphic sequence and no significant inversions in the sequence have been observed. This is further supported by the photoluminescence dating results, indicating the validity of the age estimates. However, there is an anomaly in the TG-HJ-2 sample, which warrants further investigation.

Table 1. Characteristics of OSL dating samples from the QSW, YSC and TG-HJ section

Sample	Depth(cm)	Disc	W.C.(%)	Dose(Gy)	Age(ka)
TG-HJ-1	285	6	5	$58.68 \pm 2.08$	$18.4 \pm 1.1$
TG-HJ-2	305	4	5	$317.52 \pm 62.15$	$107.5 \pm 21.7$
TG-HJ-3	335	18	5	$68.47 \pm 2.03$	$18.9 \pm 1.1$
TG-HJ-4	405	6	5	$110.65 \pm 17.82$	$28.9 \pm 4.9$

### 4.2 EMMA result

EMMA was conducted on the particle size data from the QSW, YSC, and TG-HJ sections of the YHV coast to gain a deeper understanding of soil sediment types. A non-parametric method was utilized to analyze the data, which allowed for a comparison of the content of each sediment horizon without revealing any significant trends in EM dynamics. The results obtained from the non-parametric method showed good agreement.

Table 2. Characteristics of EMs from the QSW, YSC and TG-HJ section

Section	EM	$R^2$	Angular deviation	EMs $R^2$	Median angular deviation
QSW	3	0.926	14	0.031	11.3
YSC	2	0.993	4.2	0.113	2.2
TG-HJ	2	0.983	6.3	0.099	4.1

In selecting the most appropriate EM model, we determined the number of EMs based on a thorough evaluation of multiple criteria, including the coefficient of determination ( $R^2$ ), mean angular deviation ( $\theta$ ), and compatibility with sedimentary genetic interpretation. Optimal models were identified by considering models with higher  $R^2$  values, lower  $\theta$  values, and a smaller number of EMs(Table 2). The QSW section was divided into 3 EMs, while the YSC and TG-HJ sections were divided into 2 EMs.(Fig. 2)

In the QSW section, 3 EMs were identified. EM1 is characterized by a combination of clay and fine sand particles with a mean grain size of  $5.52 \mu\text{m}$  and a broad, smooth frequency curve with the

lowest peak. This indicates the formation of secondary clay minerals after sediment deposition, possibly influenced by East Asian summer winds. EM2, dominated by fine sand particles with a mean grain size of 96.53  $\mu\text{m}$ , represents material transported by valley winds from near-source fluvial deposits. Finally, EM3 is characterized by coarse sand particles with a mean grain size of 241.84  $\mu\text{m}$  and likely represents coarse-grained sediment transported by valley winds and slope-deposited debris from near-source fluvial areas.

In the YSC section, EM1 is dominated by coarse sands with an average grain size of 26.73  $\mu\text{m}$  and is believed to be the result of material transported by valley winds from nearby fluvial sources and slopes. The sediment is thought to have been affected by late climate change-related leaching. EM2, on the other hand, is comprised mainly of fine sands with an average grain size of 82.08  $\mu\text{m}$  and is believed to have a similar origin as the EM2 in the QSW section.

In the TG-HJ section, EM1 consists mainly of fine sediment with an average grain size of 19.02  $\mu\text{m}$  and has the same origin as EM1 in the YSC section. EM2 is dominated by coarse fines with an average grain size of 50.08  $\mu\text{m}$  and is believed to have been transported by East Asian winter winds over short distances at low altitudes (Table 3).

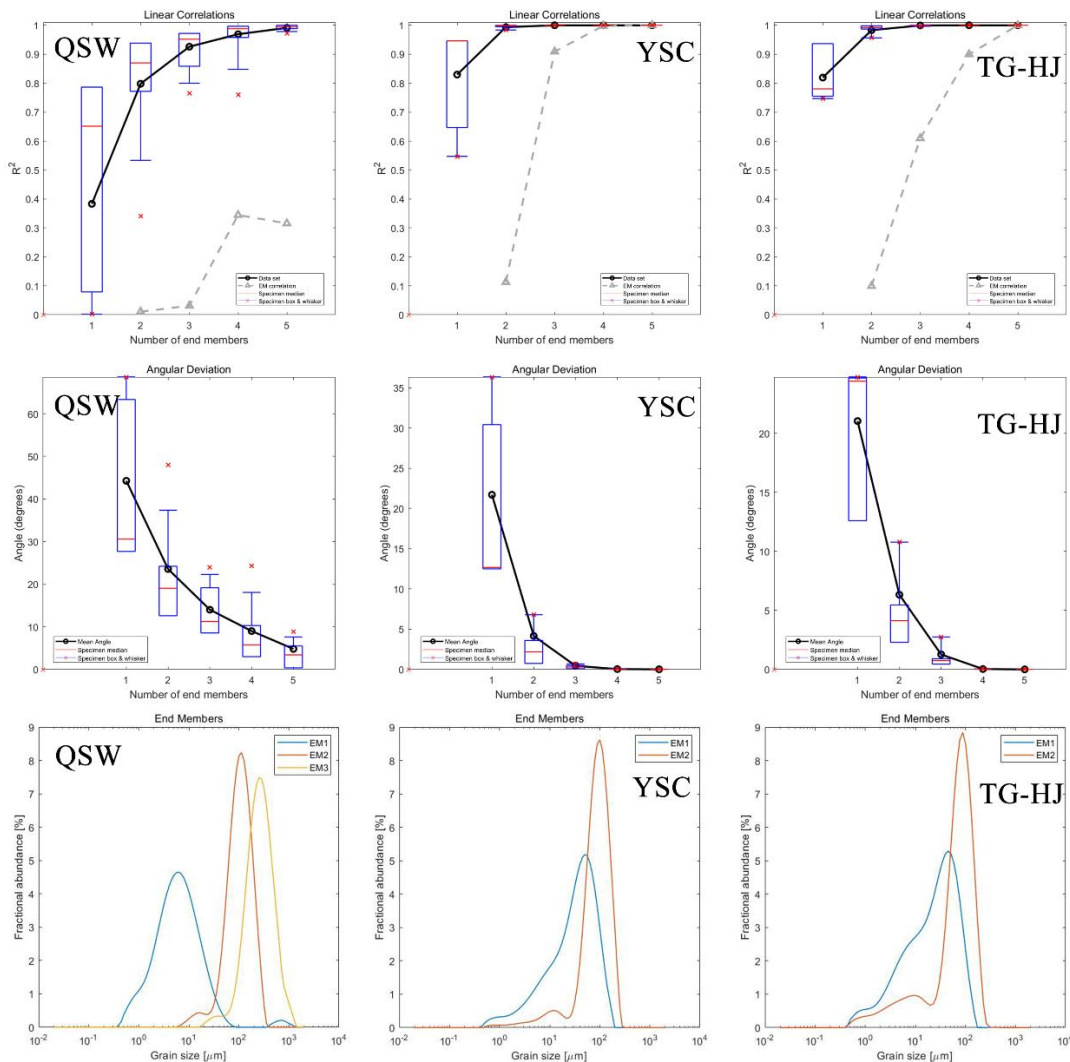


Fig. 2 End-member modelling results of grain-size data of the QSW and YSC and TG-HJ sections and the grain-size distribution curves for the modelled end members based on the 2 EMs for the YSC and TG-HJ sections, the 3 EMs for the QSW section.

In the QSW section, high values for EM1, EM2, and EM3 can be found in the SWD layer of each paleoflood stagnant sediment, suggesting that they primarily come from surface soil sediments

on both sides of the river valley carried by the erosion of the YHV during storm floods(Fig. 3). In the YSC and TG-HJ sections, EM1 represents sediment from river flood suspended sediment under a high-water level stagnant environment, while EM2 represents river diffuse beach alluvium shaped by the hydrodynamic actions of the river in the river channel.

Table 3. Grain size parameters for EMs of the QSW, YSC and TG-HJ section

Section	No.	Mz( $\mu$ m)	Sigma	Skewness	Kurtosis
QSW	EM1	5.52	2.8	-0.03	1.04
	EM2	96.53	1.8	-0.11	1.06
	EM3	241.84	1.9	-0.04	1.04
YSC	EM1	26.73	3.1	-0.33	1.06
	EM2	82.08	2	-0.28	1.54
TG-HJ	EM1	19.02	3.4	-0.29	0.93
	EM2	50.08	3.1	-0.52	1.76

### 5. Discussion

The study of soil sediments in the YHV is essential for understanding the history of environmental change and surface processes in the region. The YSC and TG-HJ sections, in particular, represent the impact of late Pleistocene mega-flood events and their influence on the landscape. The QSW section, on the other hand, offers valuable insights into the most recent Holocene flood event and its impact on the sedimentary record.

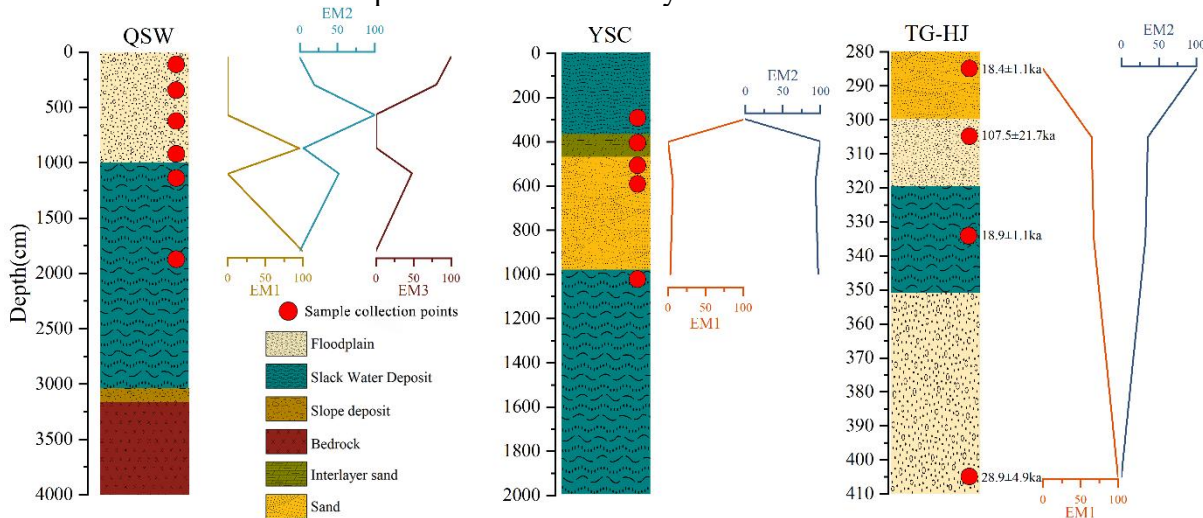


Fig. 3 The stratigraphy, dating and EMs of the QSW, YSC and TG-HJ section

The origin and provenance of the soil sediments in the QSW, YSC and TG-HJ sections in the YHV hold important clues to understanding the processes shaping the surface of the area. The Late Pleistocene period was marked by significant climatic fluctuations and changes, and the YHV experienced two mega-flood events between 28.9 and 18.4 ka, resulting in the formation of two Floodplain layers, TG-HJ and an OSL age anomaly. These deposits were mainly derived from the erosion of the watershed surface by heavy rainfall and floods and represent the long-distance transport and sorting of river sediments. In addition, the Earth's climate underwent another phase of rapid change and a large flood event took place in the YHV, leading to the formation of a 2m-thick SWD deposit in the QSW section.

By exploring the sources and geographies of soil sediments in these 3 sections, scientists can gain a better understanding of the role of flood events in shaping the landscape, as well as the long-distance transport and deposition of sediment in the region[21].

In addition, the sedimentary record in the YHV is also important for reconstructing the regional climate and environmental change during different time periods[22]. The presence of floodplain layers, for example, can be used to infer changes in rainfall patterns and the strength of flooding events[23]. The OSL age anomaly, on the other hand, provides evidence for a period of rapid climate change that has implications for the global climate system[24].

In conclusion, the study of soil sediments in the YHV is crucial for advancing our understanding of environmental change, surface processes, and regional climate in the region.

## 6. Summary

In conclusion, through the analysis of representative samples from various levels of the riverbank sections in the YHV, we have successfully applied the EMMA method and combined it with OSL dating to effectively uncover the complex deposition processes of the paleofloods in the region since the Late Pleistocene. Our findings provide valuable insights into the sedimentary evolution of the YHV.

(1) In this study, representative samples were collected from various levels of riverbank sections in the YHV and analyzed through EMMA. Results showed that 3 EMs were extracted from the QSW section and 2 from the YSC and TG-HJ sections. Through a comprehensive evaluation of the macroscopic properties, component content and other factors, it was found that the SWD in paleoflood stagnant sediment likely originated from the high water level stagnant environment of sediment carried by river floods, while the river diffuse beach alluvium represented sediment in the river channel under the influence of river hydrodynamics.

(2) The Late Pleistocene periods in the YHV riverbank saw a diversity of sediment dynamics for each soil depositional horizon. This study revealed that these periods were influenced by storm floods and climate change, with particularly heavy rainfall and flood events occurring during periods of sudden climate change or transition to climate deterioration. This was often due to unstable conditions in the East Asian monsoon atmospheric circulation and increased precipitation variability in the region. Specifically, three major flood events were identified in the YHV between 28.9 ka-18.4 ka, coinciding with global climate transitions and extreme anomalies.

## Acknowledgements

This study was supported by Natural Science Foundation of Qinghai Provincial Science and Technology Department (2021-ZJ-749).

## References

- [1] Li S, Wang Z, Zhang Y. Crop cover reconstruction and its effects on sediment retention in the Tibetan Plateau for 1900–2000[J]. *Journal of Geographical sciences*, 2017, 27: 786-800.
- [2] Dong J, Zhang Z, Liu B, et al. Spatiotemporal variations and driving factors of habitat quality in the loess hilly area of the Yellow River Basin: A case study of Lanzhou City, China[J]. *Journal of Arid Land*, 2022, 14(6): 637-652.
- [3] Chen Q, Yang L E, Luo J, et al. The 300 years cropland changes reflecting climate impacts and social resilience at the Yellow River–Huangshui River Valley, China[J]. *Environmental Research Letters*, 2021, 16(6): 065006.
- [4] Chen J, Li G J. Geochemical studies on the source region of Asian dust[J]. *Science China Earth Sciences*, 2011, 54: 1279-1301.
- [5] Dietze M, Schulte P, Dietze E. Application of end-member modelling to grain-size data: Constraints and limitations[J]. *Sedimentology*, 2022, 69(2): 845-863.
- [6] Liang X, Niu Q, Qu J, et al. Applying end-member modeling to extricate the sedimentary environment of yardang strata in the Dunhuang Yardang National Geopark, northwestern China[J]. *Catena*, 2019, 180: 238-251.

- [7] Barnes J B, Ehlers T A. End member models for Andean Plateau uplift[J]. *Earth-Science Reviews*, 2009, 97(1-4): 105-132.
- [8] Ralston K D, Birbilis N. Effect of grain size on corrosion: a review[J]. *Corrosion*, 2010, 66(7): 075005-075005-13.
- [9] Yu S Y, Colman S M, Li L. BEMMA: a hierarchical Bayesian end-member modeling analysis of sediment grain-size distributions[J]. *Mathematical Geosciences*, 2016, 48: 723-741.
- [10] IJmker J, Stauch G, Dietze E, et al. Characterisation of transport processes and sedimentary deposits by statistical end-member mixing analysis of terrestrial sediments in the Donggi Cona lake catchment, NE Tibetan Plateau[J]. *Sedimentary Geology*, 2012, 281: 166-179.
- [11] Bøtter-Jensen L, McKeever S W S, Wintle A G. *Optically stimulated luminescence dosimetry*[M]. Elsevier, 2003.
- [12] Bowman S. *Radiocarbon dating*[M]. Univ of California Press, 1990.
- [13] Ely L L, Baker V R. Reconstructing paleoflood hydrology with slackwater deposits: Verde River, Arizona[J]. *Physical Geography*, 1985, 6(2): 103-126.
- [14] Patton P C, Baker V R, Kochel R C. *Slack-water deposits: a geomorphic technique for the interpretation of fluvial paleohydrology*[M]//Adjustments of the fluvial system. Routledge, 2020: 225-253.
- [15] CHEN R, ZHOU Q, LIU F, et al. Contribution of climate change to food yield in Yellow River-Huangshui River Valley[J]. *HUBEI AGRICULTURAL SCIENCES*, 2018, 57(12): 114.
- [16] Wang T, Yan J, Cheng X, et al. Irrigation influencing farmers' perceptions of temperature and precipitation: a comparative study of two regions of the Tibetan Plateau[J]. *Sustainability*, 2020, 12(19): 8164.
- [17] Wang Q, Liu S, Liu Y, et al. Effects of urban agglomeration and expansion on landscape connectivity in the river valley region, Qinghai-Tibet Plateau[J]. *Global Ecology and Conservation*, 2022, 34: e02004.
- [18] Wang X L, Lu Y C, Wintle A G. Recuperated OSL dating of fine-grained quartz in Chinese loess[J]. *Quaternary Geochronology*, 2006, 1(2): 89-100.
- [19] Wang X L, Wintle A G, Lu Y C. Testing a single-aliquot protocol for recuperated OSL dating[J]. *Radiation measurements*, 2007, 42(3): 380-391.
- [20] Konert M, Vandenberghe J E F. Comparison of laser grain size analysis with pipette and sieve analysis: a solution for the underestimation of the clay fraction[J]. *Sedimentology*, 1997, 44(3): 523-535.
- [21] Blott S J, Pye K. GRADISTAT: a grain size distribution and statistics package for the analysis of unconsolidated sediments[J]. *Earth surface processes and Landforms*, 2001, 26(11): 1237-1248.
- [22] Sochan A, Bieganski A, Ryzak M, et al. Comparison of soil texture determined by two dispersion units of Mastersizer 2000[J]. *International Agrophysics*, 2012, 26(1).
- [23] Peng Y, Wang Q, Wang H, et al. Does landscape pattern influence the intensity of drought and flood?[J]. *Ecological Indicators*, 2019, 103: 173-181.
- [24] Carling P A. The Noon Hill flash floods; July 17th 1983. Hydrological and geomorphological aspects of a major formative event in an upland landscape[J]. *Transactions of the Institute of British Geographers*, 1986: 105-118.